

## Synthesis, Structure, and Polymorphism Studies in Amine-Templated Open-Framework Zinc Phosphites

Sukhendu Mandal and Srinivasan Natarajan\*

Framework Solids Laboratory, Solid State and Structural Chemistry Unit, Indian Institute of Science, Bangalore 560012, India

Received February 21, 2008

Five new zinc phosphites,  $[\text{C}_{10}\text{N}_4\text{H}_{26}][\text{Zn}_2(\text{HPO}_3)_4] \cdot 2\text{H}_2\text{O}$ , **1**,  $[\text{C}_{10}\text{N}_4\text{H}_{26}][\text{Zn}_5(\text{H}_2\text{O})_4(\text{HPO}_3)_6] \cdot 4\text{H}_2\text{O}$ , **2**,  $[\text{C}_{10}\text{N}_4\text{H}_{26}][\text{Zn}_4(\text{HPO}_3)_6] \cdot 2\text{H}_2\text{O}$ , **3**,  $[\text{C}_{10}\text{N}_4\text{H}_{26}][\text{Zn}_4(\text{HPO}_3)_6] \cdot 2\text{H}_2\text{O}$ , **4**, and  $[\text{Zn}_2(\text{HPO}_3)_2(\text{C}_{10}\text{N}_4\text{H}_{24})]$ , **5**, were synthesized employing solvo/hydrothermal reactions in the presence of 1,4-bis (3-aminopropyl) piperazine (APPIP). Single crystal X-ray diffraction studies indicate that all the compounds form a hierarchy of structures. While the structures **1** and **2** are low-dimensional, **3–5** have three-dimensional connectivity.  $\text{ZnO}_4$  and  $\text{HPO}_3$  units form a 4-membered ring and are connected through their corners forming a one-dimensional chain structure in **1**. **2** has one-dimensional ladders connected by  $\text{ZnO}_2(\text{H}_2\text{O})_4$  octahedral units forming a layer with 4- and 8-membered apertures. Compounds **3** and **4** have similar molecular formulae and connectivity, which makes them polymorphic in nature. The amine molecules exist in *gauche* and *all-trans* form in **3** and **4**, respectively. The amine molecule binds with the zinc center in **5** and acts as a pillar between the two zinc phosphite layers. The present study outlines the possible role of synthesis parameters for the isolation of a number of different structures by employing a single amine molecule, APPIP. The observation of polymorphic structures along with the interconvertibilities of one of the phases is important and noteworthy. The  $^{31}\text{P}$  chemical shifts observed in NMR studies, consistent with the single crystal data, have been correlated with the valence sum values of the oxygen that are bound with the distinct phosphorus.

### Introduction

Compounds exhibiting open-framework structures constitute an important family.<sup>1</sup> Research in this area continues to be attractive for their many applications, both actual as well as potential.<sup>1a,c</sup> Though most of the reported compounds belong to the family of phosphates, recent research has clearly shown that it is profitable to investigate other systems as well. Of the many compounds that have been prepared,<sup>1c</sup> the phosphite based ones appear to show structural diversity and versatility similar to that of the phosphates. Of these, the zinc phosphites are an important family of compounds exhibiting zero-,<sup>2</sup> one-,<sup>3</sup> two-<sup>4</sup> and three-dimensionally<sup>5</sup> extended structures. The zinc phosphites, in general, are prepared employing hydrothermal methods in the presence of organic amines.

One of the compelling reasons for research in this area is to look for newer structures and in some cases to investigate the close structural relationships and possible transformations between the structures within a family of compounds.

- (2) (a) Fan, J.; Slebodnick, C.; Hanson, B. E. *Inorg. Chem. Commun.* **2006**, 9, 103–106. (b) Lin, Z.-E.; Fan, W.; Gu, J.; Okubo, T. *J. Solid State Chem.* **2007**, 180, 981–987. (c) Harrison, W. T. A.; Yeates, R. M.; Philips, M. L. F.; Nenoff, T. M. *Inorg. Chem.* **2003**, 42, 1493–1498.
- (3) (a) Mandal, S.; Natarajan, S. *Solid State Sci.* **2006**, 8, 388–396. (b) Hu, L.; Fan, J.; Slebodnick, C.; Hanson, B. E. *Inorg. Chem.* **2006**, 45, 7681–7688. (c) Suhua, S.; Wei, Q.; Guanghua, L.; Li, Y.; Hongming, B. E.; Jianing, X.; Guangshan, Z.; Tianyou, S.; Shilun, Q. *J. Solid State Chem.* **2004**, 177, 3038–3044. (d) Harrison, W. T. A. *Int. J. Inorg. Mater.* **2001**, 3, 187–189. (e) Krikpatrick, A.; Harrison, W. T. A. *Solid State Sci.* **2004**, 6, 593–598.
- (4) (a) Fu, W.; Shi, Z.; Zhang, D.; Li, G.; Dai, Z.; Chen, X.; Feng, S. *J. Solid State Chem.* **2003**, 174, 11–18. (b) Philips, M. L. F.; Nenoff, T. M.; Thompson, C. T.; Harrison, W. T. A. *J. Solid State Chem.* **2002**, 167, 337–343. (c) Lin, Z.-E.; Zhang, J.; Zheng, S.-T.; Yang, G.-Y. *Solid State Sci.* **2004**, 6, 371–376. (d) Liu, L.; Liu, Y.; Li, G.; Chen, C.; Bi, M.; Pang, W. *J. Solid State Chem.* **2006**, 179, 1311–1316. (e) Zeng, Q.-X.; Ke, R.-R.; Xiang, Y.; Zhang, X.-W. *Z. Anorg. Allg. Chem.* **2005**, 631, 3066–3069. (f) Zhang, D.; Yue, H.; Shi, Z.; Feng, S. *Solid State Sci.* **2005**, 7, 1256–1260. (g) Zhong, Y.-J.; Chen, Y.-M.; Sun, Y.-Q.; Yang, G.-Y. *Z. Anorg. Allg. Chem.* **2005**, 631, 1957–1960.

\* To whom correspondence should be addressed. E-mail: snatarajan@sscu.iisc.ernet.in.

(1) (a) Cheetham, A. K.; Ferey, G.; Loiseau, T. *Angew. Chem., Int. Ed.* **1999**, 39, 3268–3292; and references therein. (b) Murugavel, R.; Walawalkar, M. G.; Dan, M.; Roesky, H. W.; Rao, C. N. R. *Acc. Chem. Res.* **2004**, 37, 763–744. (c) Maspoeh, D.; Ruiz-Molina, D.; Veciana, J. *Chem. Soc. Rev.* **2007**, 36, 770–818.

**Table 1.** Synthesis Conditions for the Compounds 1–5

mole ratio	synthesis condition			initial pH	final pH	yields (%)	composition
	temp (°C)	time (h)					
ZnO:4H <sub>3</sub> PO <sub>3</sub> :2APPIP:25THF:75H <sub>2</sub> O	75, rt	72, 96		7	7	45	[C <sub>10</sub> N <sub>4</sub> H <sub>26</sub> ][Zn <sub>2</sub> (HPO <sub>3</sub> ) <sub>4</sub> ]·2H <sub>2</sub> O, <b>1</b> <sup>a</sup>
ZnO:2HCl:2H <sub>3</sub> PO <sub>3</sub> :1.5APPIP:100H <sub>2</sub> O	75	72		6.5	6.5	70	[C <sub>10</sub> N <sub>4</sub> H <sub>26</sub> ][Zn <sub>5</sub> (H <sub>2</sub> O) <sub>2</sub> (HPO <sub>3</sub> ) <sub>8</sub> ]·4H <sub>2</sub> O, <b>2</b>
ZnO:2HCl:4H <sub>3</sub> PO <sub>3</sub> :CH <sub>3</sub> COOH:2APPIP:25THF:75H <sub>2</sub> O	75	72		6	6	80	[C <sub>10</sub> N <sub>4</sub> H <sub>26</sub> ][Zn <sub>4</sub> (HPO <sub>3</sub> ) <sub>6</sub> ]·2H <sub>2</sub> O, <b>3</b>
ZnO:2HCl:2H <sub>3</sub> PO <sub>3</sub> :APPIP:100H <sub>2</sub> O	150	72		5	5	75	[C <sub>10</sub> N <sub>4</sub> H <sub>26</sub> ][Zn <sub>4</sub> (HPO <sub>3</sub> ) <sub>6</sub> ]·2H <sub>2</sub> O, <b>4</b>
ZnO:2H <sub>3</sub> PO <sub>3</sub> :4APPIP:100H <sub>2</sub> O	75	72		10.5	10.5	80	[Zn(HPO <sub>3</sub> ) <sub>2</sub> (C <sub>10</sub> N <sub>4</sub> H <sub>24</sub> )], <b>5</b>
ZnO:2HCl:2.5H <sub>3</sub> PO <sub>3</sub> :APPIP:100H <sub>2</sub> O	75	96		2	2	80	[Zn <sub>2</sub> (H <sub>2</sub> O) <sub>4</sub> (HPO <sub>3</sub> ) <sub>2</sub> ]·H <sub>2</sub> O, <sup>b</sup>

<sup>a</sup> Impure phase. <sup>b</sup> This phase was reported by Ortiz-Avila et al.<sup>26</sup>

Recently, it has been shown that the structural study toward the understanding of polymorphism in framework structures can give rise to new insights especially in the role of weak interactions. Polymorphism, as defined by McCrone, is “a solid crystalline phase of a given compound with the same molecular formula existing in at least two different arrangements in the solid state”.<sup>6</sup> Lieberworth et al. reported the formation of two solvatomorphs in hydrated zinc phosphate (hoepite), Zn<sub>3</sub>(PO<sub>4</sub>)<sub>2</sub>·4H<sub>2</sub>O.<sup>7</sup> This study has brought out the importance of hydrogen-bond interactions in the formation of two different polymorphic structures. Polymorphism in amine-templated framework structures is not common, even though a large number of closely related structures have been known. In the family of phosphites, there have been some attempts in identifying polymorphic structures. Thus, α-[H<sub>3</sub>N(CH<sub>2</sub>)<sub>6</sub>NH<sub>3</sub>][Zn<sub>3</sub>(HPO<sub>3</sub>)<sub>4</sub>]<sup>4a</sup> and β-[H<sub>3</sub>N(CH<sub>2</sub>)<sub>6</sub>NH<sub>3</sub>]-[Zn<sub>3</sub>(HPO<sub>3</sub>)<sub>4</sub>]<sup>5g</sup> have been prepared using 1,6-diaminohexane. The structures of α-[H<sub>2</sub>N(CH<sub>2</sub>)<sub>2</sub>NH<sub>2</sub>]<sub>0.5</sub>[ZnHPO<sub>3</sub>]<sup>5c</sup> and β-[H<sub>2</sub>N(CH<sub>2</sub>)<sub>2</sub>NH<sub>2</sub>]<sub>0.5</sub>[ZnHPO<sub>3</sub>]<sup>5k</sup> have ethylenediamine bonded with the Zn-center.

We have been interested in the study of the formation of different zinc phosphite phases by the use of one particular organic amine by varying the synthetic parameters. Our earlier study on zinc phosphates indicated the possibility of isolating many different framework structures by using the same organic amine in the synthesis mixture.<sup>8</sup> For the study of the zinc phosphite phases, we have used 1,4-bis (3-aminopropyl) piperazine (APPIP) under a variety of synthesis conditions. Our investigations resulted in the isolation of five different zinc phosphite structures of varying dimensionali-

ties. Thus, [C<sub>10</sub>N<sub>4</sub>H<sub>26</sub>][Zn<sub>2</sub>(HPO<sub>3</sub>)<sub>4</sub>]·2H<sub>2</sub>O, **1**, is one-dimensional, [C<sub>10</sub>N<sub>4</sub>H<sub>26</sub>][Zn<sub>5</sub>(H<sub>2</sub>O)<sub>2</sub>(HPO<sub>3</sub>)<sub>8</sub>]·4H<sub>2</sub>O, **2**, is two-dimensional, and [C<sub>10</sub>N<sub>4</sub>H<sub>26</sub>][Zn<sub>4</sub>(HPO<sub>3</sub>)<sub>6</sub>]·2H<sub>2</sub>O, **3**, [C<sub>10</sub>N<sub>4</sub>H<sub>26</sub>]-[Zn<sub>4</sub>(HPO<sub>3</sub>)<sub>6</sub>]·2H<sub>2</sub>O, **4**, and [Zn<sub>2</sub>(HPO<sub>3</sub>)<sub>2</sub>(C<sub>10</sub>N<sub>4</sub>H<sub>24</sub>)], **5**, have three-dimensionally extended structures. Of these, compound **3** and **4** have identical framework formulae, very nearly the same structural features, and can be classified as polymorphic structures. We have also been able to show that it is possible to transform one of the polymorphic structures to the other one by subtle heat treatments. In this paper, we present the synthesis, structure, polymorphism studies, and characterizations of all the zinc phosphite phases.

## Experimental Section

The zinc phosphites **1–5** were synthesized under hydrothermal conditions starting from a mixture containing the source of zinc salt, H<sub>3</sub>PO<sub>3</sub>, and/or CH<sub>3</sub>COOH and 1,4-bis (3-aminopropyl) piperazine, (APPIP). The various synthesis conditions employed in the present study are presented in Table 1. In all the cases, the reaction mixtures were homogenized for ~30 min at room temperature and heated in a 7 mL PTFE-lined stainless steel acid digestion bomb (final fill factor ~40%) at varying time and temperature. The resulting products, which predominantly contained good-quality colorless single crystals, suitable for single crystal X-ray diffraction, were filtered and washed thoroughly with deionized water. Thus, rod like (**1**, **5**) and plate-like (**2–4**) crystals were obtained. The products during the preparation of **1** were found to contain unknown impurities, and in spite of many attempts, we were not able to prepare **1** in pure form. Hence, other than the single crystal structure studies, we were not able to characterize this compound satisfactorily.

Initial characterizations were carried out by elemental analysis, energy dispersive X-ray analysis (EDAX), powder X-ray diffraction (XRD), thermogravimetric analysis (TGA), and IR spectroscopic studies. Elemental analysis of the crystals was carried out using a CHNS analyzer (ThermoFinnigan FLASH EA 1112 CHNS analyzer). Elemental analysis calcd (%) for **2**: C 10.43, H 4.02, N 4.86; found: C 10.54, H 4.27, N 5.04; elemental analysis calcd (%) for **3**: C 12.28, H 3.68, N 5.73; found: C 13.00, H 4.00, N 5.47; elemental analysis calcd (%) for **4**: C 12.28, H 3.68, N 5.73; found: C 12.12, H 3.85, N 5.02; elemental analysis calcd (%) for **5**: C 24.45, H 5.33, N 11.40; found C 24.06, H 5.72, N 11.3. An EDAX analysis on many single crystals indicated an Zn:P ratio of 5:6 for **2**, 2:3 for **3** and **4**, 1:1 for **5**, respectively, consistent with the single crystal X-ray data.

The powder XRD patterns were recorded on crushed single crystals in the 2θ range 5–50° using Cu Kα radiation (Philips X'pert Pro). The XRD patterns of compounds **2–5** indicated that the products were pure and consistent with the XRD patterns simulated from the single crystal structure (see Supporting Information, Figures S1, S2, and S3). The XRD patterns of the two

- (5) (a) Linag, J.; Li, J.; Yu, J.; Chen, P.; Fang, Q.; Sun, F.; Xu, R. *Angew. Chem., Int. Ed.* **2006**, *45*, 2546–2548. (b) Liang, J.; Wang, Y.; Lu, J.; Xu, R. *Chem. Commun.* **2003**, 882–883. (c) Rodgers, J. A.; Harrison, W. T. A. *Chem. Commun.* **2000**, 2385–2386. (d) Chen, L.; Bu, X. *Inorg. Chem.* **2006**, *45*, 4654–4660. (e) Pan, J.-X.; Zheng, S.-T.; Yang, G.-Y. *Microporous Mesoporous Mater.* **2004**, *75*, 129–133. (f) Lin, Z.-E.; Zhang, J.; Zheng, S.-T.; Yang, G.-Y. *Microporous Mesoporous Mater.* **2004**, *68*, 65–70. (g) Holtby, A. S.; Harrison, W. T. A.; Yilmaz, V. T.; Buyukgungor, O. *Solid State Sci.* **2007**, *9*, 149–154. (h) Harrison, W. T. A.; Phillips, M. L. F.; Nenoff, T. M. *J. Chem. Soc., Dalton Trans.* **2001**, 2459–2461. (i) Pan, J.-X.; Zheng, S.-T.; Yang, G.-Y. *Cryst. Growth Des.* **2005**, *5*, 237–242. (j) Harrison, W. T. A. *J. Solid State Chem.* **2001**, *160*, 4–7. (k) Gordon, L. E.; Harrison, W. T. A. *Acta Crystallogr.* **2004**, *C60*, m637–m639. (l) Yang, Y.; Zhao, Y.; Yu, J.; Wu, S.; Wang, R. *Inorg. Chem.* **2008**, *47*, 769–771. (m) Lai, Y.-L.; Lii, K.-H.; Wang, S.-L. *J. Am. Chem. Soc.* **2007**, *129*, 5350–5351.
- (6) McCrone, W. C. In *Physics and Chemistry of the Organic Solid State*; Fox, D., Labes, M. M., Weissberger, A., Eds.; Wiley-Interscience: New York, 1965; Vol. 2, pp 725–767.
- (7) Herschke, L.; Enkelmann, V.; Liberworth, I.; Wegner, G. *Chem.-Eur. J.* **2004**, *10*, 2795–2803.
- (8) Choudhury, A.; Natarajan, S.; Rao, C. N. R. *Inorg. Chem.* **2000**, *39*, 4295–4304.

**Table 2.** Crystal Data and Structure Refinement Parameters for Compounds **1–5**

	<b>1</b>	<b>2</b>	<b>3</b>	<b>4</b>	<b>5</b>
empirical formula	C <sub>10</sub> H <sub>34</sub> N <sub>4</sub> O <sub>14</sub> P <sub>4</sub> Zn <sub>2</sub>	C <sub>10</sub> H <sub>48</sub> N <sub>4</sub> O <sub>26</sub> P <sub>6</sub> Zn <sub>5</sub>	C <sub>10</sub> H <sub>36</sub> N <sub>4</sub> O <sub>20</sub> P <sub>6</sub> Zn <sub>4</sub>	C <sub>10</sub> H <sub>36</sub> N <sub>4</sub> O <sub>20</sub> P <sub>6</sub> Zn <sub>4</sub>	C <sub>10</sub> H <sub>26</sub> N <sub>4</sub> O <sub>6</sub> P <sub>2</sub> Zn <sub>2</sub>
formula weight	689.06	1153.28	976.79	976.79	491.06
crystal system	triclinic	triclinic	monoclinic	monoclinic	monoclinic
space group	<i>P</i> (−1) (No. 2)	<i>P</i> (−1) (No. 2)	<i>P</i> 2 <sub>1</sub> / <i>n</i> (No. 14)	<i>P</i> 2 <sub>1</sub> / <i>n</i> (No. 14)	<i>P</i> 2 <sub>1</sub> / <i>c</i> (No. 14)
crystal size (mm)	0.14 × 0.10 × 0.08	0.16 × 0.10 × 0.08	0.20 × 0.16 × 0.12	0.16 × 0.10 × 0.12	0.20 × 0.10 × 0.08
<i>a</i> (Å)	7.72(3)	9.924(4)	9.749(12)	10.430(2)	13.581(3)
<i>b</i> (Å)	9.32(3)	10.077(5)	10.336(13)	9.520(2)	8.319(18)
<i>c</i> (Å)	9.79(3)	10.795(5)	15.526(19)	15.992(4)	7.817(17)
α (°)	107.56(6)	88.017(7)	90.000	90.000	90.000
β (°)	107.49(5)	75.681(7)	94.936(2)	90.516(3)	97.341(3)
γ (°)	92.86(6)	64.925(6)	90.000	90.000	90.000
volume (Å <sup>3</sup> )	633.0(4)	944.3(7)	1558.9(3)	1587.8(6)	876.0(3)
<i>Z</i>	2	2	4	4	4
ρ <sub>calcd</sub> (gcm <sup>−3</sup> )	1.797	2.028	2.083	2.041	1.846
μ (mm <sup>−1</sup> )	2.216	3.476	3.434	3.371	2.955
θ range (deg)	2.68 to 24.71	1.95 to 28.10	2.37 to 27.98	2.32 to 27.39	2.88 to 28.00
reflection collected	2553	7939	17819	12147	7382
unique reflections	1517	4212	3709	3291	2065
number of parameters	125	264	200	210	109
goodness of fit	0.959	1.009	1.256	1.034	1.092
<i>R</i> index [ <i>I</i> > 2σ( <i>I</i> )]	<i>R</i> <sub>1</sub> = 0.0906, <i>wR</i> <sub>2</sub> = 0.1746	<i>R</i> <sub>1</sub> = 0.0522, <i>wR</i> <sub>2</sub> = 0.1388	<i>R</i> <sub>1</sub> = 0.0584, <i>wR</i> <sub>2</sub> = 0.1041	<i>R</i> <sub>1</sub> = 0.0332, <i>wR</i> <sub>2</sub> = 0.0859	<i>R</i> <sub>1</sub> = 0.0246, <i>wR</i> <sub>2</sub> = 0.0692
largest diff. peak and hole e Å <sup>−3</sup>	0.452 and −0.552	1.869 and −1.625	0.587 and −0.654	0.721 and −1.118	0.814 and −0.367

polymorphic phases **3** and **4** appear to be quite similar but show subtle variations (see Supporting Information, Figure S2).

TGA studies have been carried out (Mettler-Toledo, TG850) in an atmosphere of air (flow rate = 50 mL/min) in the temperature range 25–850 °C (heating rate = 5 °C/min). For **2**, the first weight loss (obsd: 15.2%) occurring in the temperature range 100–175 °C corresponds to the loss of lattice and coordinated water molecules (calcd 12.5%) (see Supporting Information, Figure S4). The second weight loss (obsd: 17.4%) in the range 325–475 °C corresponds to the loss of the amine molecules (calcd: 17.5%). The TGA studies of the polymorphic structures **3** and **4**, carried out in nitrogen, indicated that the weight loss behavior is more or less identical with minor variations (see Supporting Information, Figure S5). Both the sample loses weight from room-temperature, and the weight loss was found to be continuous up to 500 °C. The observed weight loss of 28.65% corresponds to the loss of the lattice–water and amine molecules from the structure (calcd: 24.39%). In oxygen atmosphere, the removal of amine molecules in **3** and **4** were found to be highly exothermic and could not be completed (the sample was being thrown out of the crucible). For **5**, the weight loss was continuous from 375 °C up to 700 °C (obsd: 38.4%), which corresponds to the loss of the amine molecules (calcd. 40.8%) (see Supporting Information, Figure S4). The final decomposition product identified by powder XRD was α-Zn<sub>2</sub>P<sub>2</sub>O<sub>7</sub> (JCPDS: 72–1702) for **2** and **5** and Zn<sub>2</sub>P<sub>2</sub>O<sub>7</sub> (JCPDS Card No. 39–0711) for the polymorphic phases **3** and **4**.

IR spectroscopic studies were carried out in the range 400–4000 cm<sup>−1</sup> using the KBr pellet method (Perkin-Elmer, SPECTRUM 1000). IR spectroscopic studies exhibited typical peaks corresponding to the amine molecule, the HPO<sub>3</sub> moiety, and the lattice–water molecule with little variations in their respective bands (see Supporting Information, Table S1, Figures S6 and S7). IR (KBr): ν<sub>s</sub> = 3515–3525 cm<sup>−1</sup> (H<sub>2</sub>O), ν<sub>s</sub> = 3015–3350 cm<sup>−1</sup> (N–H), ν<sub>s</sub> = 2850–3075 cm<sup>−1</sup> (C–H)<sub>asym</sub>, ν<sub>s</sub> = 2825–2970 cm<sup>−1</sup> (C–H)<sub>sym</sub>, ν<sub>s</sub> = 2370–2408 cm<sup>−1</sup> (P–H), δ<sub>as</sub> = 1620–1642 cm<sup>−1</sup> (H<sub>2</sub>O), ν<sub>s</sub> = 1655–1690 cm<sup>−1</sup> (N–H), δ<sub>s</sub> = 1460–1480 cm<sup>−1</sup> (C–H), δ<sub>s</sub> = 1405–1430 cm<sup>−1</sup> (C–N), ν<sub>as</sub> = 1023–1140 cm<sup>−1</sup> (P–O), δ<sub>as</sub> = 985–1050 cm<sup>−1</sup> (P–H), ν<sub>s</sub> = 865–1010 cm<sup>−1</sup> (P–O), δ<sub>s</sub> = 570–610 cm<sup>−1</sup> (P–O), δ<sub>as</sub> = 450–500 cm<sup>−1</sup> (P–O).

**Solid-State MAS NMR Studies.** Solid state nuclear magnetic resonance (NMR) experiments were performed on a Bruker AVIII

500 spectrometer operating at 11.7 T with a resonance frequency of 202.47 MHz for <sup>31</sup>P. A Bruker 4 mm CPMAS probe was used for the experiments. The <sup>31</sup>P MAS spectra were recorded using standard cross-polarization (CP) procedures and high proton decoupling, employing magic angle spinning (MAS) frequency of 10kHz. In a typical experiment, rf fields of 100 kHz were used, and the chemical shifts are reported relative to 85% H<sub>3</sub>PO<sub>4</sub> as the external standard.

**Single-Crystal Structure Determination.** A suitable crystal for all compounds was carefully selected under a polarizing microscope and glued to a thin glass fiber. The single crystal diffraction data were collected on a Bruker AXS Smart Apex CCD diffractometer at 293(2) K. The X-ray generator was operated at 50 kV and 35 mA using Mo Kα (λ = 0.71073Å) radiation. Data were collected with ω scan width of 0.3°. A total 606 frames were collected in three different settings of φ (0°, 90°, 180°) keeping the sample-to-detector distance fixed at 6.03 cm and the detector position (2θ) fixed at −25°. Pertinent experimental details of the structure determination of **1–5** are presented in Table 2.

The data were reduced using SAINTPLUS,<sup>9</sup> and an empirical absorption correction was applied using the SADABS program.<sup>10</sup> The crystal structure was solved by direct methods using SHELXS97 and refined using SHELXL97 present in the WinGx suite of programs (Version 1.63.04a).<sup>11</sup> One of the oxygen atoms, O(8), in **4** was found to be disordered over two sites with a site occupancy factor (SOF) of 0.5. Because of the disorder, we have not been able to locate the hydrogen atoms to lattice–water molecule of **1**, **3**, and **4** and to the P atoms of **4** that are bonded with O(8). The location of hydrogen positions for these molecules was not feasible. The hydrogen atom on the P–H group of other compounds and the hydrogen positions of the amine molecules in the compounds **1–5** were located in the difference Fourier map. For the final refinement, the hydrogen atoms were placed in geometrically ideal positions and refined using the riding mode. We have employed isotropic refinement for the disordered atoms. The last cycles of

(9) SMART (V 5.628), SAINT (V 6.45a), XPREP, SHELXTL; Bruker AXS Inc.: Madison, WI, 2004.

(10) Sheldrick, G. M. *Siemens Area Correction Absorption Correction Program*; University of Göttingen: Göttingen, Germany, 1994.

(11) Sheldrick, G. M. *SHELXL-97 Program for Crystal Structure Solution and Refinement*; University of Göttingen: Göttingen, Germany, 1997.

the refinement included atomic positions, anisotropic thermal parameters for all the non-hydrogen atoms, and isotropic thermal parameters for all the hydrogen atoms. Full-matrix-least-squares structure refinement against  $F^2$  was carried out using the WINGX<sup>12</sup> package of programs. The poor quality of the data of **1** may be attributed to the fact that the crystal is not robust and tends to decompose during the process of data collection.

CCDC-676510–676514 contains the crystallographic data for **1–5**. These data can be obtained free of charge from The Cambridge Crystallographic Data Centre (CCDC) via [www.ccdc.cam.ac.uk/data\\_request/cif](http://www.ccdc.cam.ac.uk/data_request/cif).

## Results

**[C<sub>10</sub>N<sub>4</sub>H<sub>26</sub>][Zn<sub>2</sub>(HPO<sub>3</sub>)<sub>4</sub>]·2H<sub>2</sub>O, **1**.** The asymmetric unit of **1** contains 17 non-hydrogen atoms, of which one Zn and two P atoms are crystallographically independent. The zinc atom is tetrahedrally coordinated with four oxygen atoms with an average bond distance of 1.908 Å, and O–Zn–O bond angles are in the range of 101.5(5)–115.0(5)°. The zinc atom makes four Zn–O–P bonds (av. 130.6°). The phosphorus atoms have two P–O–Zn bonds and one terminal P–O bond with the P–O bond distances and O–P–O bond angles in the expected range (Table 3 and Supporting Information, Table S2).

The structure of **1** consists of strictly alternating ZnO<sub>4</sub> and HPO<sub>3</sub> units connected through the oxygen vertices to form a four-membered ring, which are connected through the corners forming a one-dimensional chain-like structure (Figure 1a). The protonated APPIP molecules are located in the interchain spaces and participate in hydrogen bond-interactions through N–H···O and C–H···O bonds, which give rise to a supramolecularly arranged layer structure (Figure 1b). The important hydrogen bond interactions are listed in Table 4.

**[C<sub>10</sub>N<sub>4</sub>H<sub>26</sub>][Zn<sub>5</sub>(H<sub>2</sub>O)<sub>4</sub>(HPO<sub>3</sub>)<sub>6</sub>]·4H<sub>2</sub>O, **2**.** The asymmetric unit of **2** contains 26 non-hydrogen atoms, of which three Zn and P atoms are crystallographically independent. Of these, Zn(1) occupy a special position (1e) with site multiplicity of 0.5. Of the three Zn atoms, the Zn(1) atom is octahedrally coordinated and the Zn(2) and Zn(3) atoms are tetrahedrally coordinated by oxygen atom neighbors with average bond distances of 2.098 Å, 1.955 Å, and 1.951 Å for Zn(1), Zn(2), and Zn(3), respectively. The O–Zn(1)–O bond angles for the octahedral Zn(1) is nearly perfect and in the range of 87.0(1)–180.0(1)°, and the tetrahedral O–Zn–O bond angles are in the range of 101.4(1)–115.4(1)°. The Zn(1) makes two Zn–O–P bonds (av. 140.9°) and possess four terminal Zn–OH<sub>2</sub> bonds while the Zn(2) and Zn(3) make four Zn–O–P bonds (av. 125.7°). All three P atoms make three P–O–Zn bonds with the P–O bond distances in the range 1.514(3)–1.527(3) Å and with the O–P–O bond angles in the range of 109.7(2)–114.1(2)° (Table 3 and Supporting Information, Table S2).

The structure of **2** consists of a network of ZnO<sub>2</sub>(H<sub>2</sub>O)<sub>4</sub>, ZnO<sub>4</sub>, and HPO<sub>3</sub> units. The Zn(2)O<sub>4</sub>, Zn(3)O<sub>4</sub> and HP(2)O<sub>3</sub>, HP(3)O<sub>3</sub> units strictly alternate and are connected through

**Table 3.** Selected Bond Distances for the Compounds **1–5**

bond	distance, (Å)	bond	distance, (Å)
Compound 1 <sup>a</sup>			
Zn(1)–O(1)	1.864(10)	P(1)–O(2)	1.400(11)
Zn(1)–O(2)	1.905(11)	P(1)–O(5)	1.416(13)
Zn(1)–O(3)	1.916(10)	P(2)–O(3)#2	1.487(10)
Zn(1)–O(4)	1.949(11)	P(2)–O(4)	1.448(10)
P(1)–O(1)#1	1.564(10)	P(2)–O(6)	1.473(14)
Compound 2 <sup>b</sup>			
Zn(1)–O(1)	2.000(3)	Zn(3)–O(10)#3	1.952(3)
Zn(1)–O(1)#1	2.000(3)	Zn(3)–O(11)#4	1.955(3)
Zn(1)–O(2)	2.101(3)	P(1)–O(1)	1.515(3)
Zn(1)–O(2)#1	2.101(3)	P(1)–O(4)	1.524(3)
Zn(1)–O(3)	2.195(3)	P(1)–O(11)	1.522(3)
Zn(1)–O(3)#1	2.195(3)	P(2)–O(6)	1.520(3)
Zn(2)–O(4)	1.946(3)	P(2)–O(8)	1.519(3)
Zn(2)–O(5)	1.954(3)	P(2)–O(10)	1.514(3)
Zn(2)–O(6)	1.957(3)	P(3)–O(5)	1.527(3)
Zn(2)–O(7)	1.964(3)	P(3)–O(7)#2	1.526(3)
Zn(3)–O(8)#2	1.949(3)	P(3)–O(9)	1.519(3)
Zn(3)–O(9)	1.949(3)		
Compound 3 <sup>c</sup>			
Zn(1)–O(1)	1.920(3)	P(1)–O(7)	1.511(4)
Zn(1)–O(2)#1	1.933(3)	P(1)–O(8)	1.521(4)
Zn(1)–O(3)	1.933(4)	P(2)–O(2)	1.511(4)
Zn(1)–O(4)	1.954(3)	P(2)–O(3)	1.514(4)
Zn(2)–O(5)#2	1.919(4)	P(2)–O(6)	1.514(4)
Zn(2)–O(6)#1	1.920(4)	P(3)–O(4)	1.544(3)
Zn(2)–O(7)#3	1.953(3)	P(3)–O(5)	1.514(4)
Zn(2)–O(8)	1.959(4)	P(3)–O(9)	1.491(4)
P(1)–O(1)	1.514(4)		
Compound 4 <sup>d</sup>			
Zn(1)–O(1)	1.907(3)	P(1)–O(6)	1.447(3)
Zn(1)–O(2)	1.915(3)	P(1)–O(8)	1.44(5)
Zn(1)–O(3)	1.935(2)	P(2)–O(2)#2	1.493(3)
Zn(1)–O(4)	1.938(2)	P(2)–O(4)	1.509(2)
Zn(2)–O(5)	1.901(3)	P(2)–O(5)	1.498(3)
Zn(2)–O(6)#1	1.915(3)	P(3)–O(1)#3	1.510(3)
Zn(2)–O(7)	1.938(3)	P(3)–O(7)	1.526(3)
Zn(2)–O(8)	1.950(5)	P(3)–O(9)	1.481(3)
P(1)–O(3)	1.493(2)		
Compound 5 <sup>e</sup>			
Zn(1)–O(1)	1.938(16)	P(1)–O(1)	1.511(16)
Zn(1)–O(2)	1.941(16)	P(1)–O(2)#2	1.515(16)
Zn(1)–O(3)#1	1.953(15)	P(1)–O(3)	1.523(16)
Zn(1)–N(1)	2.021(18)		

<sup>a</sup> Symmetry transformations used to generate equivalent atoms for **1**: #1,  $-x + 2, -y + 1, -z$ ; #2,  $-x + 1, -y + 1, -z$ ; #3,  $-x + 1, -y, -z$ .

<sup>b</sup> Symmetry transformations used to generate equivalent atoms for **2**: #1,  $-x + 1, -y + 1, -z$ ; #2,  $-x + 2, -y + 1, -z$ ; #3,  $x, y - 1, z$ ; #4,  $x + 1, y - 1, z$ ; #5,  $x, y + 1, z$ .

<sup>c</sup> Symmetry transformations used to generate equivalent atoms for **3**: #1,  $-x + 3/2, y - 1/2, -z + 1/2$ ; #2,  $-x + 1, -y, -z$ ; #3,  $-x + 1/2, y - 1/2, -z + 1/2$ . <sup>d</sup> Symmetry transformations used to generate equivalent atoms for **4**: #1,  $x - 1, y, z$ ; #2,  $-x + 1/2, y + 1/2, -z + 1/2$ ; #3,  $x - 1/2, -y + 1/2, z + 1/2$ . <sup>e</sup> Symmetry transformations used to generate equivalent atoms for **5**: #1,  $-x, -y + 1, -z + 1$ ; #2,  $x, -y + 3/2, z + 1/2$ .

the oxygen vertices forming the four-membered ring, which are connected through their edges forming a one-dimensional ladder-like structure (Figure 2a). The ladders are linked through HP(1)O<sub>3</sub> and Zn(1)O<sub>2</sub>(H<sub>2</sub>O)<sub>4</sub> units to form the layer structure with 4 and 8-membered apertures (Figure 2b), which are stacked one over the other in a AAAA... fashion (Figure 2c). The organic cations and the water molecules occupy the interlayer spaces and interact with the framework through N–H···O and O–H···O hydrogen-bond interactions (Figure 2c and Table 4).

**[C<sub>10</sub>N<sub>4</sub>H<sub>26</sub>][Zn<sub>4</sub>(HPO<sub>3</sub>)<sub>6</sub>]·2H<sub>2</sub>O, **3** and **4**.** The asymmetric unit of **3** and **4** contain 22 non-hydrogen atoms. Of these,

(12) Farrugia, J. L. *J. App. Crystallogr.* **1999**, *32*, 837–838.

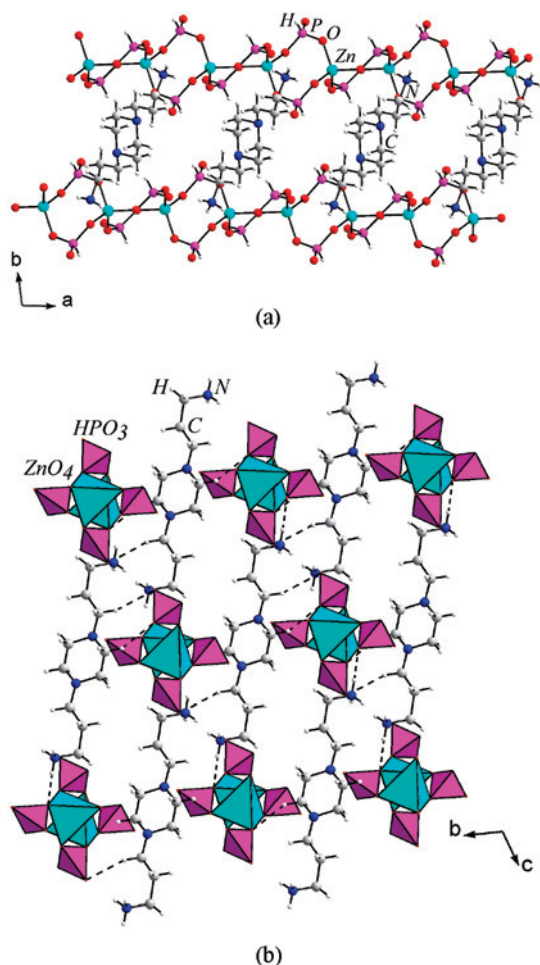


**Figure 1.** (a) Structure of **1**,  $[\text{C}_{14}\text{N}_4\text{H}_{26}][\text{Zn}_2(\text{HPO}_3)_4] \cdot 2\text{H}_2\text{O}$ , showing the one-dimensional chain along with the APPIP molecules. (b) The two-dimensional structure formed by the hydrogen bond interactions between the amine and the zinc phosphite units. Dotted lines represent the possible hydrogen bond interactions.

two Zn and three P atoms are crystallographically independent. The zinc atoms are tetrahedrally coordinated by four oxygen atom neighbors with an average Zn–O bond distance of 1.936 Å for **3** and 1.924 Å for **4**. The O–Zn–O bond angles are in the range of 94.6(2)–122.7(2)°. All the zinc atoms make four Zn–O–P linkages (av. = 130.6° for **3** and 137.2° for **4**). P(1) and P(2) have three P–O–Zn bonds, and P(3) makes two P–O–Zn bonds and possesses one terminal P–O linkage. The P–O bond distances are in the range of 1.442(5)–1.544(3) Å, and the O–P–O bond angles are in the range of 104.0(2)–122.5(3)° (Table 3 and Supporting Information, Table S2).

The structural connectivity in both compounds is similar, consisting of  $\text{ZnO}_4$  and  $\text{HPO}_3$  units connected through their vertices. The  $\text{HP}(1)\text{O}_3$  and  $\text{HP}(2)\text{O}_3$  are connected with the  $\text{ZnO}_4$  units giving rise to a two-dimensional structure with apertures bound by 8-T atoms (T = Zn, P) (Figure 3a,b). Similar two-dimensional layers have been observed in other zinc phosphite structures as well.<sup>4c</sup> The layers are further connected by an  $\text{HP}(3)\text{O}_3$  unit forming the observed three-dimensional structure, with one-dimensional channels bound by 8-T atoms (Figure 4a,b). This, in a way, is similar to the pillaring of layers by phosphite groups. Pillaring of layers

**Table 4.** Important Observed Hydrogen Bond Interactions in the Compounds **1–4**

D–H···A	D–H (Å)	H···A (Å)	D···A (Å)	D–H···A (°)
Compound 1				
N(2)–H(11)···O(6)	0.89	1.94	2.72(2)	146
N(2)–H(12)···O(1)	0.89	1.95	2.78(2)	155
C(1)–H(2)···O(3)	0.97	2.29	3.16(3)	151
C(3)–H(5)···O(100)	0.97	2.53	3.50(3)	177
C(3)–H(6)···O(3)	0.97	2.36	3.20(3)	144
C(3)–H(6)···O(6)	0.97	2.56	3.48(3)	157
Compound 2				
intra O(2)–H(2A)···O(7)	0.95	2.07	3.002(5)	166
intra O(2)–H(2B)···O(10)	0.94	1.91	2.849(5)	179
intra O(3)–H(3A)···O(5)	0.94	1.93	2.824(6)	157
O(3)–H(3B)···N(2)	0.94	1.99	2.900(5)	160
N(1)–H(12)···O(4)	0.89	2.39	3.275(5)	170
O(100)–H(101)···O(9)	0.85	2.21	3.019(7)	159
O(200)–H(202)···O(100)	0.84	1.98	2.810(10)	170
Compound 3				
N(1)–H(1)···O(9)	0.89	1.99	2.781(5)	148
N(1)–H(2)···O(9)	0.89	1.87	2.757(5)	171
N(1)–H(3)···O(7)	0.89	2.07	2.945(5)	165
N(2)–H(10)···O(4)	0.91	1.83	2.732(5)	170
C(3)–H(8)···O(2)	0.97	2.38	3.228(6)	145
C(3)–H(9)···O(1)	0.97	2.57	3.524(6)	170
C(4)–H(11)···O(8)	0.97	2.58	3.540(6)	171
Compound 4				
N(1)–H(1)–O(9)	0.89	1.89	2.760(4)	165
N(1)–H(2)–O(3)	0.89	1.99	2.874(4)	170
N(1)–H(3)–O(4)	0.89	2.04	2.926(4)	172
N(2)–H(10)–O(7)	0.91	1.88	2.751(4)	159

by phosphate groups have been observed earlier in open-framework phosphates.<sup>13</sup> The 1,4-bis (3-aminopropyl) piperazine molecules and extra-framework water molecules occupy the channels. The two structures can, in fact, be considered as truly polymorphic in nature. N–H···O and C–H···O type hydrogen bond interactions have been observed in **3**, and only N–H···O type interaction were observed in **4** (Table 4).

**[Zn<sub>2</sub>(HPO<sub>3</sub>)<sub>2</sub>(C<sub>10</sub>N<sub>4</sub>H<sub>24</sub>)], 5.** The asymmetric unit of **5** contains 12 non-hydrogen atoms, of which one Zn and P atoms are crystallographically independent. The zinc atom is tetrahedrally coordinated with three oxygen atoms of the phosphite group and one nitrogen atom of the amine molecule with an average bond distance of Zn–O/N = 1.963 Å and O–Zn–O/N bond angles are in the range of 98.24(7)–116.51(7)°. The zinc atom makes three Zn–O–P bonds (av. 130.76°) and one Zn–N–C bond. The P atom makes three P–O–Zn linkages with P–O bond distances in the range of 1.511(2)–1.523(2) Å, and the O–P–O bond angles are in the range of 111.8(1)–112.7(9)° (Table 3 and Supporting Information, Table S2).

The structure of **5** consists of a network of strictly alternating  $\text{ZnO}_3\text{N}$  tetrahedral and  $\text{HPO}_3$  units, connected through their vertices to form a layered structure with 4- and 8-membered apertures (Figure 5a). The layer structure is similar to that observed in the structure of **3** and **4**. The layers in **5**, however, are covalently connected by 1,4-bis (3-aminopropyl) piperazine, which acts as a pillar, complet-

(13) Choudhury, A.; Natarajan, S.; Rao, C. N. R. *Chem. Commun.* **1999**, 1305–1306.

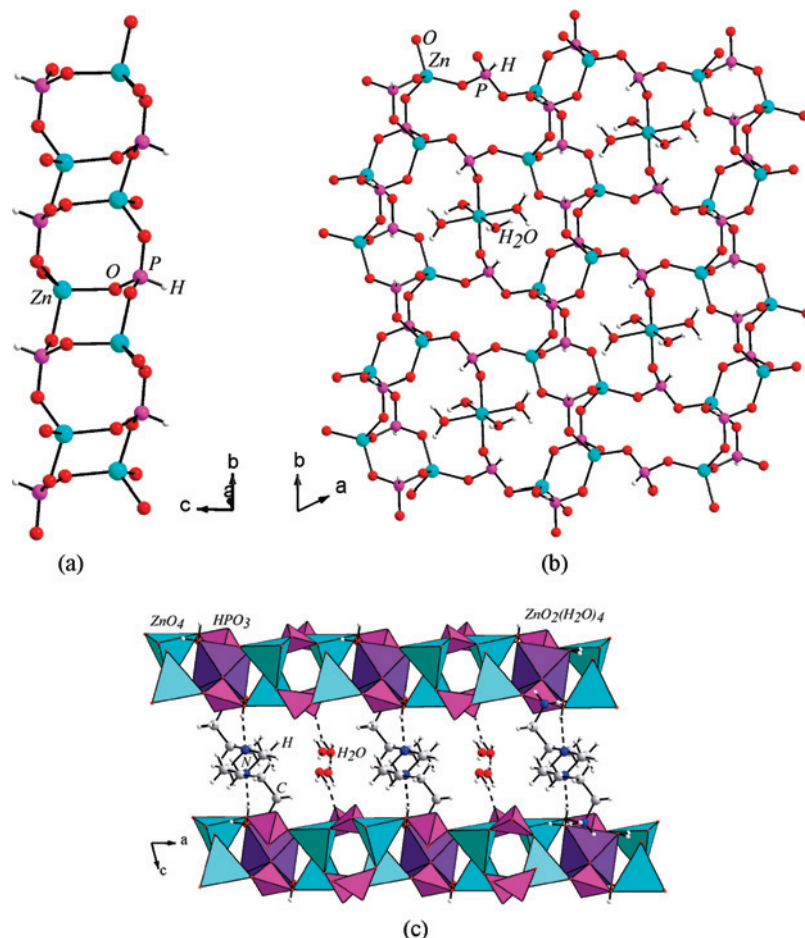


**Figure 2.** (a) One-dimensional ladder in **2**,  $[\text{C}_{10}\text{N}_4\text{H}_{26}][\text{Zn}_5(\text{H}_2\text{O})_4(\text{HPO}_3)_6] \cdot 4\text{H}_2\text{O}$ . (b) The two-dimensional layer structure with 4- and 8-membered apertures in **2** in the  $ab$  plane. Note that the layer is formed by the connectivity between the ladders and the octahedral Zn. (c) The arrangement of layers of **2** in the  $ac$  plane.

ing the three-dimensional structure (Figure 5b). The pillaring of such layers by amine molecules has been observed recently in open-framework zinc phosphites.<sup>5c</sup>

**Polymorphism in Open-Framework Zinc Phosphites, 3 and 4.** As mentioned earlier, the zinc phosphites  $[\text{C}_{10}\text{N}_4\text{H}_{26}][\text{Zn}_4(\text{HPO}_3)_6] \cdot 2\text{H}_2\text{O}$ , **3**, and  $[\text{C}_{10}\text{N}_4\text{H}_{26}][\text{Zn}_4(\text{HPO}_3)_6] \cdot 2\text{H}_2\text{O}$ , **4**, can be considered as polymorphic structures. Among the wide variety of organically templated inorganic framework structures, the isolation of polymorphic structures is rare. Recently, Harrison et al. showed that in the zinc phosphite structures the  $\beta$ - $[\text{H}_3\text{N}(\text{CH}_2)_6\text{NH}_3][\text{Zn}_3(\text{HPO}_3)_4]$ <sup>5g</sup> structure complements the  $\alpha$ - $[\text{H}_3\text{N}(\text{CH}_2)_6\text{NH}_3][\text{Zn}_3(\text{HPO}_3)_4]$  reported by Feng et al.<sup>4a</sup> The two structures are closely related and polymorphic in nature. Another polymorphic structure with the  $\alpha$ - and  $\beta$ - form is the zinc phosphite structure,  $[\text{H}_2\text{N}(\text{CH}_2)_2\text{NH}_2]_{0.5}[\text{ZnHPO}_3]$ , where the ethylenediamine molecules are bonded with Zn metal and act as a pillar connecting the zinc phosphite layers.<sup>5c,k</sup> The polymorphic structures are prepared by modifying the synthesis conditions significantly. Thus,  $\text{Zn}(\text{OAc})_2/5\text{H}_3\text{PO}_3/3(1,6\text{-DAH})$  was heated in 2 mL of  $\text{H}_2\text{O}$  at 180 °C for 5 days to obtain the  $\alpha$ - form,  $[\text{H}_3\text{N}(\text{CH}_2)_6\text{NH}_3][\text{Zn}_3(\text{HPO}_3)_4]$ ; whereas  $\text{ZnO}/2\text{H}_3\text{PO}_3/1(1,6\text{-DAH})$  was heated in 25 mL of  $\text{H}_2\text{O}$  at 80 °C for 2 days to obtain the  $\beta$ -form,  $[\text{H}_3\text{N}(\text{CH}_2)_6\text{NH}_3][\text{Zn}_3(\text{HPO}_3)_4]$ . Similarly,  $\text{ZnO}/$

$\text{H}_3\text{PO}_3/en$  was heated in 18 mL of water (23 mL autoclave) at 150 °C for 2 days to obtain the  $\alpha$ -form,  $[\text{H}_2\text{N}(\text{CH}_2)_2\text{NH}_2]_{0.5}[\text{ZnHPO}_3]$ ; and  $2\text{ZnO}/3\text{H}_3\text{PO}_3/2en$  was heated in 20 mL  $\text{H}_2\text{O}$  (60 mL autoclave) at 80 °C for 2 days to obtain the  $\beta$ -form,  $[\text{H}_2\text{N}(\text{CH}_2)_2\text{NH}_2]_{0.5}[\text{ZnHPO}_3]$ . In our present studies,  $[\text{C}_{10}\text{N}_4\text{H}_{26}][\text{Zn}_4(\text{HPO}_3)_6] \cdot 2\text{H}_2\text{O}$ , **3**, was prepared at 75 °C using a (THF +  $\text{H}_2\text{O}$ ) mixture, and  $[\text{C}_{10}\text{N}_4\text{H}_{26}][\text{Zn}_4(\text{HPO}_3)_6] \cdot 2\text{H}_2\text{O}$ , **4**, was obtained at 150 °C using  $\text{H}_2\text{O}$ . It appears that the changes in the reaction composition, especially the source for the metal ion or the solvent, could play a important role in the formation of different but closely related phases.<sup>5g</sup>

As described above, closely related polymorphic structures have been isolated, but the reactivities of such polymorphic phases have not been investigated in any great detail. A detailed study of the reactivities of the polymorphic structures of zinc phosphate phases,  $[\text{NMe}_4][\text{ZnP}_2\text{O}_8\text{H}_3]$ , specially the interconvertibilities between the two phases, have been investigated by modifying the temperature and other reaction conditions by Wiebecke and Marler.<sup>14</sup> Because we have also obtained two polymorphic phases, **3** and **4**, we sought to investigate the relative stabilities of the two structures and the possibility of inter convertibility between them.

(14) Wiebecke, M.; Marler, B. *Solid State Sci.* **2004**, *6*, 213–223.

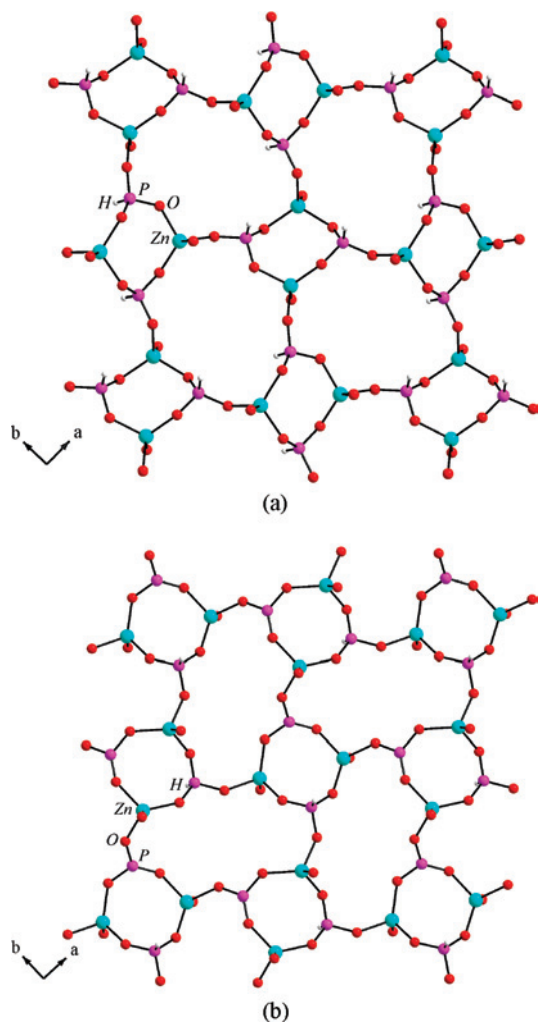


**Figure 3.** View of the layer structure formed by four- and eight-membered rings in the polymorphic structure,  $[\text{C}_{10}\text{N}_4\text{H}_{26}][\text{Zn}_4(\text{HPO}_3)_6] \cdot 2\text{H}_2\text{O}$ , (a) in **3** and (b) in **4**.

In the structures of **3** and **4**, we find the amine molecules present in two different orientations, which may be a clue for the possible origin in the differences between the two structures. In **3**, the amine molecules are in *gauche* form, and in **4** they exist in *all-trans* form (see Supporting Information, Figure S8). This difference in the orientation of the amine molecules is also reflected in their ability to form hydrogen bond interactions. Thus, in **3** we have both  $\text{N}-\text{H}\cdots\text{O}$  and  $\text{C}-\text{H}\cdots\text{O}$  interactions, whereas only  $\text{N}-\text{H}\cdots\text{O}$  interactions are observed in **4** (Table 4). A careful IR spectroscopic study reveals that in **3** and **4** the extra-framework water molecules are also involved in the formation of the hydrogen bonds [ $\text{O}(100)-\text{O}(8) = 2.931\text{\AA}$  in **3** and  $\text{O}(100)-\text{O}(9) = 2.765\text{\AA}$  in **4**]. In addition, the differences in the orientation of the amine molecules are also observed in the IR spectra (see Supporting Information, Table S1 and Figure S7). The  $\text{C}-\text{H}$  stretching frequencies of the methylene group normally are affected by the conformation of the  $\text{C}-\text{C}$  bonds and are shifted to higher frequencies in the presence of a *gauche* disorder.<sup>15</sup> This is due to the fact that the conformation energy of the *gauche* form is higher

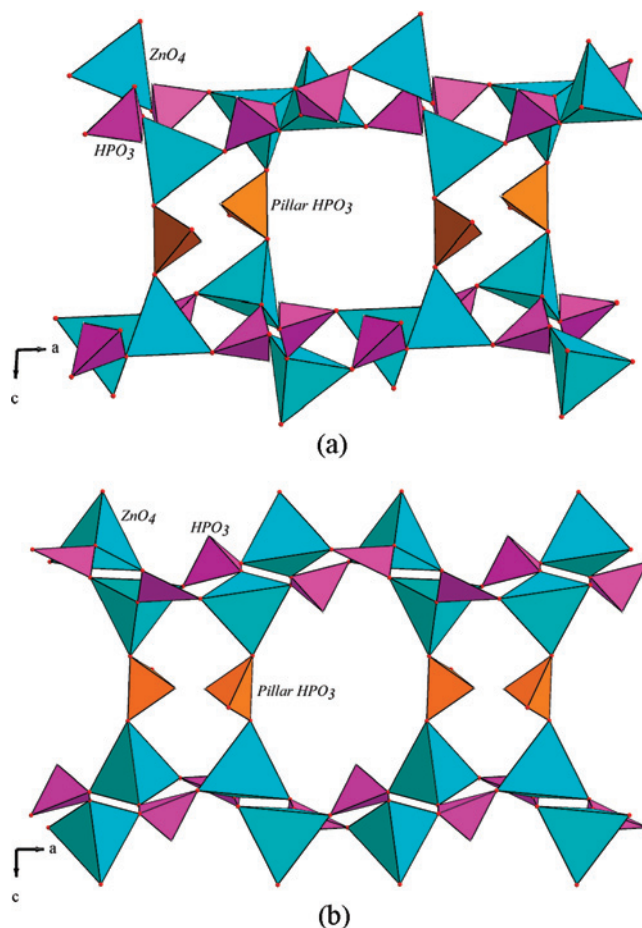


**Figure 4.** Connectivity between the layers via an  $\text{HPO}_3$  unit, forming the three-dimensional structure in the polymorphic structure,  $[\text{C}_{10}\text{N}_4\text{H}_{26}][\text{Zn}_4(\text{HPO}_3)_6] \cdot 2\text{H}_2\text{O}$ , (a) in **3** and (b) in **4**.

than that of the *all-trans* form.<sup>16</sup> Both the symmetric and asymmetric stretching frequencies of the  $\text{C}-\text{H}$  modes in **4** appear at a lower value compared to that in **3**. The methylene wagging was observed at  $1390\text{ cm}^{-1}$  for **3** while no IR bands were observed in this region for **4** (see Supporting Information, Table S1 and Figure S7).<sup>15c</sup>

To understand the energy difference between the two forms (*gauche* and *all-trans*) of the amine, APPIP, in **3** and **4**, we have also performed quantum chemical calculations using the density functional theory at the B3LYP/6-31G+(d,p) level available in the Gaussian program suite.<sup>17</sup> The conformational interactions of the amine molecule were studied by calculating the full potential energy surface (PES) across the torsional angle ( $\varphi$ ). The calculated energy profile for the free amine molecule is shown in Figure 6. As can be noted, the *cis* form ( $\varphi = 0^\circ$ ) is  $5.2\text{ kcal/mol}$  higher in energy compared to the *all-trans* conformation ( $\varphi = 180^\circ$  and  $-180^\circ$ ). Indeed, such an energy barrier for the rotation is

- (15) (a) Snyder, R. G.; Strauss, H. L. *J. Phys. Chem.* **1982**, *86*, 5145–5150. (b) Snyder, R. G.; Hsu, S. L.; Krimm, S. *Spectrochim. Acta, Part A* **1978**, *34A*, 395–406. (c) Barman, S.; Venkataraman, N. V.; Vasudevan, S.; Seshadri, R. *J. Phys. Chem. B* **2003**, *107*, 1857–1883.
- (16) Nasipuri, D. *Stereochemistry of Organic Compounds, Principles and Applications*; New Age International (P) Limited Publishers: New Delhi, 2002.
- (17) (a) *Gaussian 03*, Revision B. 05; Gaussian Inc.: Pittsburg, PA, 2003. (b) Dewarz, M. J. S.; Zebisch, E. G.; Healy, E. F.; Stewart, J. J. P. *J. Am. Chem. Soc.* **1985**, *107*, 3902–3909.

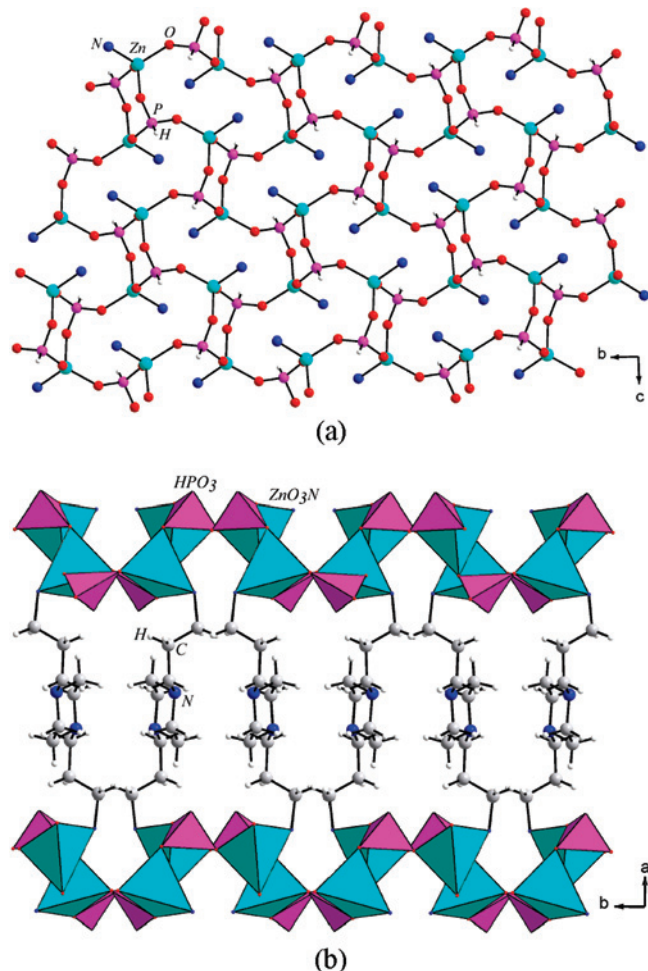


**Figure 5.** (a) View of the layer formed by four- and eight-membered rings in  $[\text{Zn}_2(\text{HPO}_3)_2(\text{C}_{10}\text{N}_4\text{H}_{24})]$ , **5**. (b) View of the three-dimensional structure showing the layers pillared by APPIP molecules in **5**.

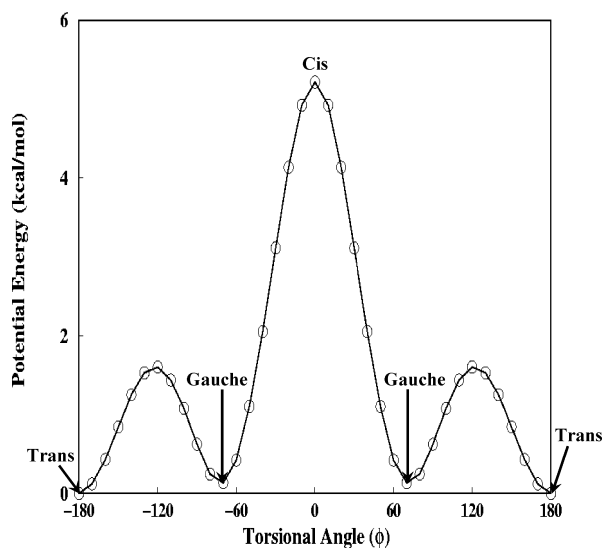


**Figure 6.** Potential energy profile for 1,4-bis(3-aminopropyl)piperazine (APPIP) molecule based on the Gaussian calculations (see text).

generally not attained under the present experimental conditions. This probably is the reason for the absence of the *cis*-form of the amine in our compounds. However, as clearly seen from the energy profile, the *gauche* form ( $\varphi = 60^\circ$  and  $-60^\circ$ ) is only 0.42 kcal/mol higher in energy compared to

the *all-trans* conformation ( $\varphi = 180^\circ$  and  $-180^\circ$ ). This is quite comparable to the thermal energy at room temperature ( $\sim 0.6$  kcal/mol). Also, note that the energy barrier between the two observed forms (*gauche* and *all-trans*) is 1.6 kcal/mol ( $\varphi = 120^\circ$  and  $-120^\circ$ ). The low energy difference between the two conformers (*gauche* and *all-trans*) probably results in the existence of both forms for the amine molecules in the two polymorphic structures that we have actually synthesized. This is possibly one of the approaches for rationalizing the formation of the two different but closely related polymorphic structures **3** and **4**.

From a structural point of view, both structures are formed by the expected building units,  $\text{ZnO}_4$  and  $\text{HPO}_3$  units. Though the individual building units in the structures are more or less regular with the bond angles, and the distances observed are comparable to those in other similar compounds, the connectivity between them creates the subtle differences. For example, the connectivity between  $\text{ZnO}_4$  and  $\text{HPO}_3$  units ( $\text{Zn}-\text{O}-\text{P}$ ) make an angle of  $130.6^\circ$  for **3** while in **4** the angle is  $137.2^\circ$ . It has been proposed that, in zeolites having similar Si/Al ratios (T atoms), the subtle variations in the T-O-T angles are one of the reasons for the observation of many different but closely related structures.<sup>18</sup> Similarly, we have the same Zn/P ratio in both **3** and **4**, but the differences in the T-O-T angles could have resulted in creating the minor differences between the two structures. The differences between the structures are also reflected in the size and shape of the 8-membered one-dimensional channels found in **3** and **4** (Figure 7).

To investigate the possible interconvertibility between **3** and **4**, we have carried out a study of the solvent-mediated transformation reactions. The pure phase of the compound **3** (0.25 g) was taken in a 7 mL PTFE-lined autoclave and heated in the presence of a THF/ $\text{H}_2\text{O}$  mixture (1.00 mL + 0.70 mL) at  $150^\circ\text{C}$  for 24 h, which resulted in **4** along with a small unidentified impurity phase ( $d = 5.87\text{\AA}$ ). This indicated that it is indeed possible to transform one of the polymorphs (**3**) to the other (**4**). Because the transformation reactions were carried out under solvothermal conditions, the possible formation of other closely related phases, if any, during the solvent mediated transformation of **3**, also was investigated by performing a time-dependent study. For this, we employed a new set of autoclaves having an identical reaction mixture as before, but the autoclaves were removed at various time intervals and the products were characterized using powder XRD (see Supporting Information, Figure S9). As can be noted, the polymorph **3** transformed into the polymorph **4** in about 4 h, along with the unidentified phase ( $d = 5.87\text{\AA}$ ). After 20 h the phase **4** appears to be fully formed with a small unidentified phase, which appears to be present even up to 24 h. The present study indicates that one of the polymorphs, **3**, can be transformed to the other phase, **4**. Our attempt to transform **4** to **3**, however, was not very successful. Though it has been possible to show the interconvertibility of polymorph **3** to polymorph **4**, we are still not clear about the possible mechanistic pathway for

(18) *Atlas of Zeolite Structure Types*; Baerlocher, Ch., Meier, W. M., Olson, D. H., Eds.; Elsevier: Amsterdam, 2001.



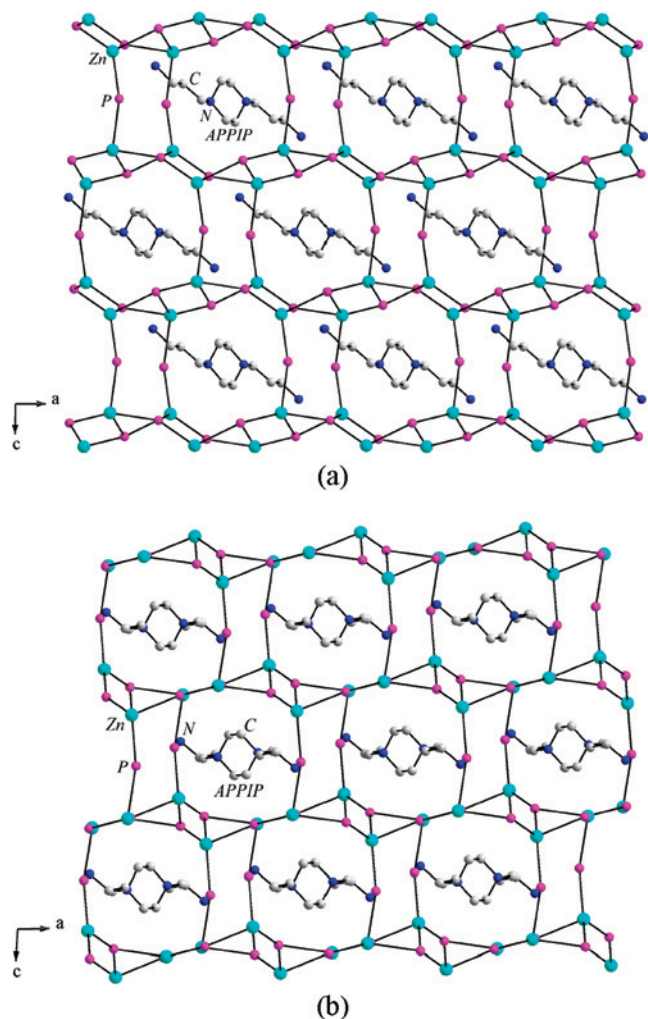


**Figure 7.** T-atoms (T = Zn, P) connectivity of the polymorphic structures (a) in **3** and (b) in **4**. Note that the *gauche* form is accommodated in **3** and the *all-trans* form in **4** (see text).

this transformation. It is likely that the dissolution followed by recrystallization could be the possible pathway. In-situ studies using synchrotron radiation, employed by O'Hare et al. to investigate some of the transformation reaction of zinc and gallium phosphates,<sup>19</sup> would be required to learn and understand the various stages of the transformation.

**Proton-Decoupled  $^{31}\text{P}$  CPMAS NMR Spectroscopic Studies.** The proton decoupled  $^{31}\text{P}$  CPMAS NMR spectroscopic studies have been carried out on a Bruker-AVIII 500 spectrometer.  $\text{H}_3\text{PO}_4$  (85%) was used as the external standard, and the chemical shifts are relative to the phosphoric acid. The observed  $^{31}\text{P}$  spectra and the number of chemical shifts observed are in complete agreement with the single crystal study for the independent phosphorus species. Thus, for **2**, three  $^{31}\text{P}$  signal were observed at 7.9, 7.3, and 6.1 ppm (see Supporting Information, Figure S10a); three signals for **3** at 2.1, 0.7, and  $-2.2$  ppm (Figure 8a); three signals for **4** at 0.2,  $-4.4$ , and  $-5.9$  ppm (Figure 8b); and one signal at 2 ppm for **5** (see Supporting Information, Figure S10b). Each signal was also accompanied by a set of spinning side

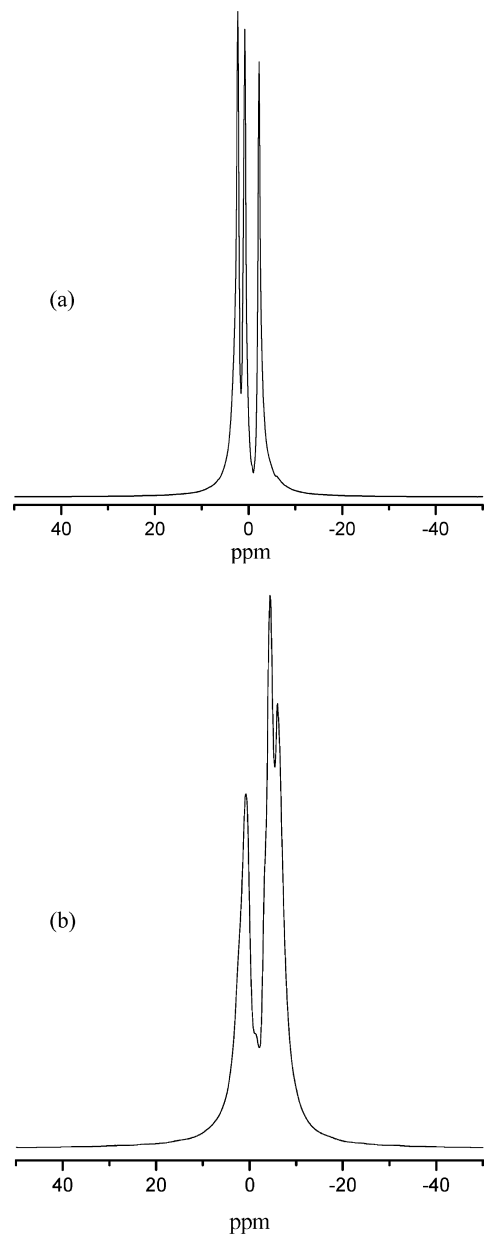


**Figure 8.**  $^{31}\text{P}$ -CPMAS NMR spectra for (a) **3** and (b) **4**.

bands. Since the internuclear distances among the P sites in all the compounds are similar (all the P atoms are connected to Zn via oxygen and there are no P–O–P linkages), the magnitude of the  $^{31}\text{P}$ – $^{31}\text{P}$  dipole coupling constants could be comparable. The two-dimensional double-quantum or exchange based NMR studies, however, may not be quite revealing with respect to the subtle interactions in the assignment of the respective phosphorus species from the NMR studies alone. The assignment, however, can be rationalized by combining the  $^{31}\text{P}$  isotropic chemical shift and the bond distances obtained from the single crystal structural data. Thus, the chemical shift values can be correlated with the bond valence sum of the oxygens that are bonded with the corresponding phosphorus.

It has been postulated and correlated that the isotropic chemical shifts of the  $^{31}\text{P}$  spectra move toward the upfield when the bond strength of the P–O bond increases.<sup>20</sup> To

(19) (a) Norquist, A. J.; O'Hare, D. *J. Am. Chem. Soc.* **2004**, *126*, 6673–6679. (b) Millange, F.; Walton, R. I.; Guillou, N.; Loiseau, T.; O'Hare, D.; Ferey, G. *Chem. Mater.* **2002**, *14*, 4448–4459.

compare and also to verify such a reasoning in our present compounds, we employed the bond valence sum method of Brown (see Supporting Information, Table S3).<sup>21</sup> Thus, for **2**, the bond valence sum of the oxygens,  $\Sigma[S(O^{2-})]$ , bonded with the phosphorus atoms P(1), P(2), and P(3) are 5.81, 5.45, and 5.37, respectively (see Supporting Information, Table S3). The observed <sup>31</sup>P peaks at 6.12, 7.34, and 7.91 ppm then must correspond to P(1), P(2), and P(3), respectively (see Supporting Information, Table S4).

The usefulness of this approach can also be employed to examine the two polymorphic structures **3** and **4** obtained in the present study. The bond valence sum values of the oxygens are 5.51, 5.60, and 5.01 for the three phosphorus species P(1), P(2), and P(3), which would correspond to the observed <sup>31</sup>P chemical shifts at 0.76, -2.16, and 2.12 ppm, respectively, in the case of compound **3** (Figure 8a). For **4**, we obtained the oxygen bond valence sum values of 6.20, 5.76, and 5.16 for the three phosphorus P(1), P(2), and P(3), which again would correspond to the observed value of the <sup>31</sup>P chemical shifts at -5.90, -4.45, and 0.28 ppm, respectively (Figure 8b).

In **3** and **4**, we observed three independent phosphorus species in the <sup>31</sup>P spectra, but the relative chemical shifts are not the same. This can be rationalized by considering the bond strength values of the oxygens in **3** and **4**. The bond strength values are larger in **4** compared to **3** leading to more negative chemical shifts in the <sup>31</sup>P spectra. It is also likely that the active participation of many oxygens in the hydrogen bond interactions in **3** would also contribute to this subtle effect. This rationalization though is not very conclusive, but it at least suggests the importance of hydrogen bonds and also the sum of the bond strengths in the relative chemical shift values observed in the <sup>31</sup>P NMR spectra.

### Comment on the Synthesis

The literature abounds with report of many open-framework structured materials prepared using a variety of organic amines as structure-directing agents.<sup>1a,c,22</sup> There have been some studies on the use of a single amine for preparing a number of different structures.<sup>8</sup> Recently, Wang and co-workers have shown that it is possible to prepare different zinc phosphate phases using the organic amine DETA<sup>23</sup> which has already been shown to give rise to three different zinc phosphate phases.<sup>24</sup> In all these studies, there has been

no correlation between the starting synthesis composition and the final solid product. In the present studies, we have prepared five different zinc phosphite phases using a single amine, APPIP, of which four are obtained as phase pure solids, with compound **1** being the exception. Most of the compounds are prepared near the neutral pH except **5**, which was obtained under basic conditions. Rao and co-workers have proposed a reasonable correlation between the pH of the starting mixture and the degree of protonation of the phosphorus species in the final solid phase product.<sup>8,25</sup> Unfortunately such studies have not been carried out in the family of phosphites. From the present study, it appears that under basic conditions, the amine molecule selectively binds with Zn (compound **5**), and similar observations have also been made in zinc phosphates.<sup>8</sup> It is to be noted that such amine binding with other metal ions are rarely observed. The formation of two polymorphic species by a small variation in the synthesis mixture indicates that the starting composition plays a crucial role in the final solid product, which agrees well with other similar observations.<sup>4a,5e,g,k,14</sup> In addition, we have also been able to show that by manipulating the reaction conditions one of the polymorphic forms (**3**) can be transformed to the other (**4**). Though solution mediated transformation of polymorphic phases has been shown in amine templated zinc phosphate structures,<sup>14</sup> this is the first such study in amine templated zinc phosphites. Though it is a little premature to generalize from the present observations, it is becoming clear that the basic pH of the reaction mixture might lead to amine bonded Zn centers, and the highly acidic conditions could result in an octahedral zinc species. Further work is necessary to investigate this aspect and to make a better correlation between the synthesis conditions and the final solid product.

**Acknowledgment.** We thank Mr. Ravi, NMR center, IISc for help with the collection of NMR data and Dr. Ayan Datta for help with the Gaussian calculations. S.N. gratefully acknowledges the generous support from the Department of Science and Technology (DST) and the Council of Scientific and Industrial Research (CSIR), Government of India, for the award of research grants and RAMANNA Fellowship. S.N. also thanks Department of Atomic Energy and Board of Research on Nuclear Sciences (DAE-BRNS), Government of India, for the award of a research grant.

**Supporting Information Available:** Tables and figures containing IR, NMR, and XRD data and selected bond angles, bond lengths, and bond strengths for compounds **1–5** (PDF). This material is available free of charge via the Internet at <http://pubs.acs.org>.

IC800333G

- (20) (a) Cheetham, A. K.; Clayden, N. J.; Dobson, C. M.; Jakeman, R. J. B. *J. Chem. Soc., Chem. Commun.* **1986**, 195–197. (b) Tang, M.-F.; Liu, Y.-H.; Chang, P.-C.; Liao, Y.-C.; Kao, H.-M.; Lii, K.-H. *Dalton Trans.* **2007**, 4523–4528.  
 (21) Brown, I. D.; Altermatt, D. *Acta Crystallogr.* **1985**, B41, 244–247.  
 (22) Rao, C. N. R.; Behera, J. N.; Dan, M. *Chem. Soc. Rev.* **2006**, 35, 375–387.  
 (23) Chang, W.-M.; Cheng, M.-Y.; Liao, Y.-C.; Chang, M.-C.; Wang, S.-L. *Chem. Mater.* **2007**, 19, 6114–6119.  
 (24) (a) Neeraj, S.; Natarajan, S.; Rao, C. N. R. *Chem. Commun.* **1999**, 165–166. (b) Neeraj, S.; Natarajan, S.; Rao, C. N. R. *Chem. Mater.* **1999**, 11, 1390–1395. (c) Neeraj, S.; Natarajan, S.; Rao, C. N. R. *New J. Chem.* **1999**, 303–308.

- (25) Rao, C. N. R.; Natarajan, S.; Choudhury, A.; Neeraj, S.; Ayi, A. A. *Acc. Chem. Res.* **2001**, 34, 80–87.  
 (26) Ortiz-Avila, C. Y.; Squattrito, P. J.; Shieh, M.; Clearfield, A. *Inorg. Chem.* **1989**, 28, 2608–2615.